

Weak antilocalization in a polarization-doped $\text{Al}_x\text{Ga}_{1-x}\text{N}/\text{GaN}$ heterostructure with single subband occupation

N. Thillozen, Th. Schäpers,^{a)} N. Kaluza, H. Hardtdegen, and V. A. Guzenko
*Institute of Thin Films and Interfaces (ISG-1) and Virtual Institute of Spin Electronics (VISel),
 Research Centre Jülich GmbH, 52425 Jülich, Germany*

(Received 30 September 2005; accepted 3 December 2005; published online 11 January 2006)

Spin-orbit scattering in a polarization-doped $\text{Al}_{0.30}\text{Ga}_{0.70}\text{N}/\text{GaN}$ two-dimensional electron gas with one occupied subband is studied at low temperatures. At low magnetic fields weak antilocalization is observed, which proves that spin-orbit scattering occurs in the two-dimensional electron gas. From measurements at various temperatures the elastic scattering time τ_{tr} , the dephasing time τ_{ϕ} , and the spin-orbit scattering time τ_{so} are extracted. Measurements in tilted magnetic fields were performed, in order to separate spin and orbital effects. © 2006 American Institute of Physics. [DOI: 10.1063/1.2162871]

GaN-based layer systems are very interesting candidates regarding the realization of future spin-based electronics (spintronics). The interest in this material for spintronics was ignited by the theoretical prediction that diluted magnetic semiconductor based on GaN should show Curie temperatures above room temperature.¹ GaN-based diluted magnetic semiconductors are promising materials for spin injection because of their expected good matching to AlGaN/GaN heterostructures. However, for a successful realization of spintronic devices an essential prerequisite is that the spin orientation can be controlled externally. A prominent example is the spin transistor proposed by Datta and Das.² Here, the spin orientation in a two-dimensional electron gas (2DEG) is controlled by a gate electrode via the Rashba spin-orbit coupling originating from a macroscopic electric field in an asymmetric quantum well.³

For semiconductor quantum wells with a large band gap channel layer, i.e., GaN, it is not obvious that the Rashba effect is sufficiently strong, because the Rashba coupling parameter α decreases with increasing band gap. However, recently it was shown theoretically that owing to the polarization field at the AlGaN/GaN heterointerface and owing to the large carrier concentration a relatively large Rashba spin-splitting energy can be expected.⁴ Experimentally information on the Rashba effect can be obtained from the characteristic beating pattern in the Shubnikov-de Haas oscillations^{5,6} or by analyzing weak antilocalization.^{7,8} For some AlGaN/GaN heterostructures a characteristic beating pattern was observed in the magnetoresistance, which was interpreted as the presence of the Rashba effect.^{9–12} In addition to the Rashba effect, the lack of inversion symmetry in zincblende-type or wurtzite-type semiconductors can also alter the spin orientation during the electron propagation (Dresselhaus term).¹³

The question to which extent spin-orbit coupling affects the electron transport in an AlGaN/GaN 2DEG is still not solved completely. One reason is, that the observation of beating effects in the Shubnikov-de Haas oscillations is not an unambiguous signature for the presence of spin-orbit coupling.^{11,14} In contrast, we focused on analyzing weak antilocalization at very low magnetic fields in a polarization-

doped AlGaN/GaN heterostructure which is a unambiguous indication of spin-orbit effects. Randomization of the spin orientation by spin-orbit scattering during the electron propagation is responsible for the presence of weak antilocalization, in contrast to weak localization where the spin orientation is conserved.^{15,16} Since only one subband is occupied in our 2DEG, contributions from intersubband scattering to the weak antilocalization could be excluded. By comparing the low-field magnetoresistance to a theoretical model the spin-orbit scattering time τ_{so} was extracted. A short τ_{so} is essential for efficient spintronic devices based on spin-orbit coupling.

The polarization-doped $\text{Al}_{0.30}\text{Ga}_{0.70}\text{N}/\text{GaN}$ heterostructure was grown by metalorganic vapor phase epitaxy on a (0001) Al_2O_3 substrate. The layer sequence is depicted in Fig. 1 [inset (a)]. Hall bar structures were prepared by dry mesa etching. Ohmic contacts of Ti/Al/Ni/Au (10 nm/200 nm/35 nm/100 nm) were annealed at 900 °C for 30 s.

Magnetotransport measurements were performed over the magnetic-field range of 0–16 T at various temperatures and in tilted magnetic fields. Figure 1 shows the longitudinal and transversal magnetoresistance at 100 mK. Pronounced Shubnikov-de Haas oscillations as well as quantum Hall steps are observed. As can be seen in Fig. 1 [inset (b)], the

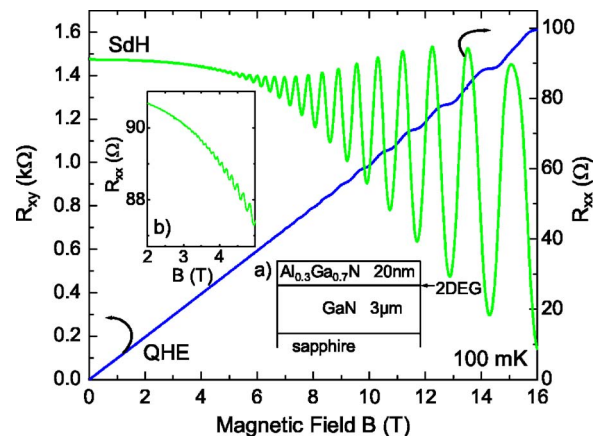


FIG. 1. (Color online) Longitudinal magnetoresistance R_{xx} and transverse magnetoresistance R_{xy} for a magnetic field oriented perpendicular to the heterointerface at 100 mK. The insets show a detail of R_{xx} at low magnetic fields and a schematic illustration of the layer sequence.

^{a)}Electronic mail: th.schaepers@fz-juelich.de

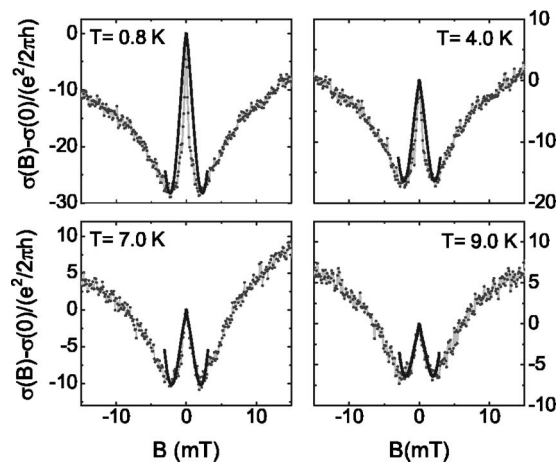


FIG. 2. (Color online) Experimental magnetoconductivity $\sigma(B) - \sigma(0)$ normalized to $e^2/2\pi h$ measured at 0.8, 4.0, 7.0, and 9.0 K (gray lines and dots). The black lines show the calculated values using the theory of Iordanskii, Lyanda-Geller, and Pikus (see Ref. 18).

Shubnikov-de Haas oscillations can be resolved down to 3 T. The clear single periodicity of the oscillations indicates that in the quantum well only a single subband is occupied. No beating pattern is observed. From the longitudinal resistance the carrier concentration and mobility were determined to be $n = 6.2 \times 10^{12} \text{ cm}^{-2}$ and $\mu = 9100 \text{ cm}^2/\text{Vs}$ at 100 mK, respectively. Up to a temperature of 12.0 K these two quantities did not change with temperature. From temperature dependent Shubnikov-de Haas measurements an effective electron mass m^* of $0.22m_e$ was extracted. Using the value of 1.17 ps for the elastic scattering time τ_{tr} , a transport mean free path $l_{tr} = 380 \text{ nm}$, and a diffusion constant $D = 0.063 \text{ m}^2/\text{s}$ were determined, which are relevant for the latter analysis of the weak antilocalization measurements.

In order to resolve spin-related effects in the electron transport studies, we measured the magnetoresistance at very low fields in the temperature range between 0.8 and 12.0 K. As can be seen in Fig. 2, close to zero magnetic field a negative slope of the magnetoconductivity $\sigma(B) - \sigma(0)$ is found for $B > 0$, which can be attributed to weak antilocalization. At $B \approx 2 \text{ mT}$ a transition to a positive slope of the magnetoconductivity attributed to weak localization is observed. If the temperature is increased the weak antilocalization peak decreases.

The fact that weak antilocalization is observed is an unambiguous sign that spin-related phenomena affect the electron transport. Since only one single subband is occupied, as indicated by the single periodicity of the Shubnikov-de Haas oscillations, we can exclude that the negative magnetoconductivity is related to intersubband scattering.¹¹ In general weak antilocalization can be due to skew scattering at impurities (Elliot-Jaffet mechanism) or due to spin randomization while propagating between scattering centers (Dyakonov-Perel mechanism). However, it was shown that for two-dimensional electron gases the Elliot-Jaffet mechanism can be neglected.¹⁷

In order to obtain detailed information about the spin relaxation, we compared the experimental curves of the magnetoconductance with theoretical calculations. In a 2DEG the Dyakonov-Perel spin relaxation can have two origins: first, the Rashba spin-orbit coupling³ and second, the Dresselhaus term.¹³ A model which takes these two mechanisms into ac-

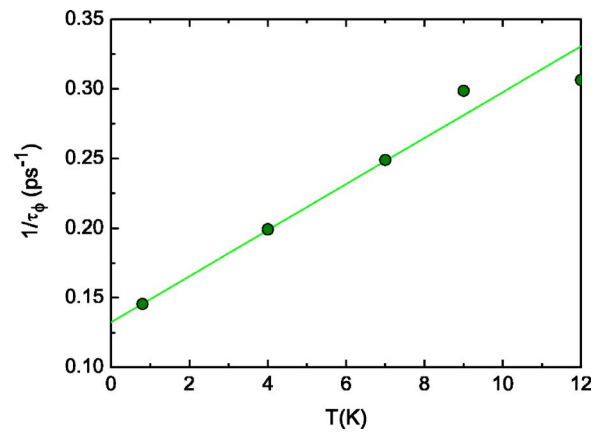


FIG. 3. (Color online) Inverse phase relaxation time $1/\tau_\phi$ as a function of the temperature. The solid line shows the linear dependence.

count was first developed by Iordanskii, Lyanda-Geller, and Pikus (ILP).¹⁸ The ILP model covers the diffusive regime, where the magnetic field is smaller than the characteristic transport field: $B_{tr} = \hbar/2el_{tr}^2$. Very recently, the ILP model has been generalized to the high-mobility regime.^{19,20}

Using the ILP model we have fitted the magnetoconductivity $\sigma(B) - \sigma(0)$, as shown in Fig. 2. The simulation was limited to fields up to $\approx 3 \text{ mT}$, in order to stay within the diffusive limit. The crystal structure of the AlGaIn/GaN heterostructures is wurtzite type. This implies that the electric field originating from the lack of inversion symmetry (Dresselhaus term) is oriented along the (0001) direction and thus parallel to the macroscopic electric field in the quantum well responsible for the Rashba effect. Therefore, we only considered the Rashba term in the ILP model quantifying both contributions. At lower temperature, i.e., 0.8 and 4.0 K, the conductance peak could not be fitted very well, we attribute this discrepancy to the different crystal lattice symmetry. From our fit we extracted a characteristic spin-orbit field of $B_{so} = 2.1 \text{ mT}$ resulting in a short spin-orbit scattering time $\tau_{so} = \hbar/4eDB_{so}$ of 1.25 ps. In the measured temperature range all fits were satisfactory for a constant value of B_{so} . The value of τ_{so} obtained from the fit is only slightly larger than the value of τ_{tr} and thus close to the limit where the ILP model can be applied. The actual value of τ_{so} in our structure thus might deviate slightly from the value extracted from the fit. Regarding the inelastic scattering time τ_ϕ , which is related to the corresponding characteristic field B_ϕ by τ_ϕ

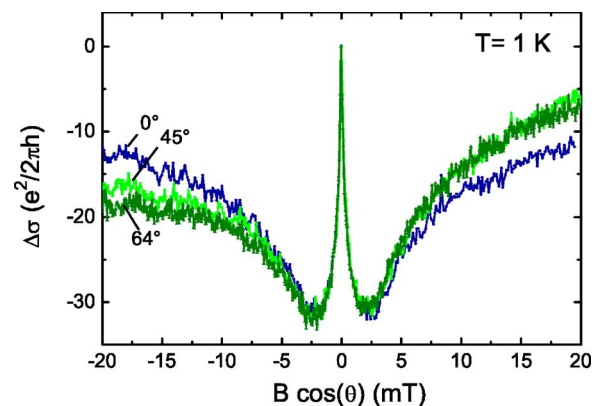


FIG. 4. (Color online) Angle-dependent measurement of weak antilocalization at 1 K.

$=\hbar/4eDB_\phi$, we found a linear increase of $1/\tau_\phi$ with temperature (Fig. 3), with values of $\tau_\phi=6.9$ and 3.3 ps at 0.8 and 12 K, respectively. The linear increase of $1/\tau_\phi$ with T can be explained by electron-electron interaction.²¹ The fact that the weak antilocalization originates from the orbital motion in the plane of the 2DEG is confirmed by measurements in tilted magnetic fields. As can be seen in Fig. 4, the weak localization and weak antilocalization features only depend on the perpendicular component of the magnetic field. No suppression of the weak antilocalization due to the contribution of the Zeeman effect was observed, as recently found in InAlAs/InGaAs heterostructures.²²

The strength of the Rashba spin splitting is usually quantified by the coupling parameter α . In our structure the contribution from the Rashba and Dresselhaus term cannot be distinguished. However, since the related electric fields are parallel one can define an effective coupling parameter $\tilde{\alpha}$, which quantifies both contributions. Using the expression⁸ $\tilde{\alpha}=\hbar/k_F\sqrt{\tau_{so}\tau_{tr}}$ we obtained a value of 8.54×10^{-13} eV m. The corresponding spin precession length $l_{so}=\hbar^2/2\tilde{\alpha}m^*$ of approximately 200 nm is relatively short, which can be attributed to the large effective mass. The short value of l_{so} extracted here is promising for the realization of small-scale spintronic devices.² However, in order to finally assess the potential of AlGaN/GaN structure for a spin transistor, measurements on gated samples are necessary so that the contributions from the controllable Rashba effect and the fixed Dresselhaus term can be distinguished.

The authors thank V. I. Litvinov and Yu. B. Lyanda-Geller for fruitful discussions.

¹T. Dietl, H. Ohno, F. Matsukura, J. Cibert, and D. Ferrand, *Science* **287**, 1019 (2000).

²S. Datta and B. Das, *Appl. Phys. Lett.* **56**, 665 (1990).

- ³E. I. Rashba, *Fiz. Tverd. Tela (Leningrad)* **2**, 1224 (1960) [*Sov. Phys. Solid State* **2**, 1109 (1960)].
- ⁴V. Litvinov, *Phys. Rev. B* **68**, 155314 (2003).
- ⁵J. Nitta, T. Akazaki, H. Takayanagi, and T. Enoki, *Phys. Rev. Lett.* **78**, 1335 (1997).
- ⁶G. Engels, J. Lange, Th. Schäpers, and H. Lüth, *Phys. Rev. B* **55**, R1958 (1997).
- ⁷T. Koga, J. Nitta, T. Akazaki, and H. Takayanagi, *Phys. Rev. Lett.* **89**, 046801 (2002).
- ⁸C. Schierholz, R. Kürsten, G. Meier, T. Matsuyama, and U. Merkt, *Phys. Status Solidi B* **233**, 436 (2002).
- ⁹I. Lo, J. K. Tsai, W. J. Yao, and P. C. Ho, *Phys. Rev. B* **65**, 161306 (2002).
- ¹⁰K. Tsubaki, N. Maeda, T. Saitoh, and N. Kobayashi, *Appl. Phys. Lett.* **80**, 3126 (2002).
- ¹¹J. Lu, B. Shen, N. Tang, D. J. Chen, H. Zhao, D. W. Liu, R. Zhang, Y. Shi, Y. D. Zheng, Z. J. Qiu, Y. S. Gui, B. Zhu, W. Yao, J. H. Chu, K. Hoshino, and Y. Arakawa, *Appl. Phys. Lett.* **85**, 3125 (2004).
- ¹²K. Cho, T.-Y. Huang, H.-S. Wang, M.-G. Lin, T.-M. Chen, C.-T. Liang, and Y. F. Chen, *Appl. Phys. Lett.* **86**, 222102 (2005).
- ¹³G. Dresselhaus, *Phys. Rev.* **100**, 580 (1955).
- ¹⁴S. Brosig, K. Ensslin, R. J. Warburton, C. Nguyen, B. Brar, M. Thomas, and H. Kroemer, *Phys. Rev. B* **60**, R13989 (1999).
- ¹⁵S. Hikami, A. I. Larkin, and Y. Nagaoka, *Prog. Theor. Phys.* **63**, 707 (1980).
- ¹⁶B. L. Al'tshuler, A. G. Aronov, A. I. Larkin, and D. E. Khmel'nitskii, *Zh. Eksp. Teor. Fiz.* **81**, 768 (1981); [*JETP Lett.* **81**, 788 (1981)].
- ¹⁷W. Knap, C. Skierbiszewski, A. Zduniak, E. Litwin-Staszewska, D. Bertho, F. Kobbi, J. L. Robert, G. E. Pikus, F. G. Pikus, S. V. Iordanskii, V. Mosser, K. Zekentes, and Yu. B. Lyanda-Geller, *Phys. Rev. B* **53**, 3912 (1996).
- ¹⁸S. V. Iordanskii, Y. B. Lyanda-Geller, and G. E. Pikus, *JETP Lett.* **60**, 206 (1994).
- ¹⁹J. B. Miller, D. M. Zumbühl, C. M. Marcus, Y. B. Lyanda-Geller, D. Goldhaber-Gordon, K. Campman, and A. C. Gossard, *Phys. Rev. Lett.* **90**, 076807 (2003).
- ²⁰L. E. Golub, *Phys. Rev. B* **71**, 235310 (2005).
- ²¹B. L. Al'tshuler, A. G. Aronov, and D. E. Khmel'nitskii, *J. Phys. C* **15**, 7367 (1982).
- ²²F. E. Meijer, A. F. Morpurgo, T. M. Klapwijk, and J. Nitta, *Phys. Rev. Lett.* **94**, 186805 (2005).